Chapter 2

Gallium Nitride-based Semiconductor Optical Amplifiers

Rintaro Koda, Hideki Watanabe and Shunsuke Kono

Additional information is available at the end of the chapter

http://dx.doi.org/10.5772/61664

Abstract

GaN-based material can potentially cover a wide spectral emission range, and laser diodes emitting in the UV, violet, blue, green, and red wavelengths have already been demonstrated and/or commercialized. GaN-based semiconductor optical amplifiers (SOAs) have the ability to boost the output power of laser diodes and thus are candidates for a broad variety of potential uses. Applications that utilize short wavelength, ultrafast pulses, including microprocessing, orthoptics, and next-generation optical storage can most benefit from GaN-based SOAs since current ultrafast pulse sources rely on large, expensive solid-state lasers. GaN-based SOAs can generate high-energy, high peak power optical pulses when used in conjunction with mode-locked laser diodes. In this chapter, the basic characteristics of these devices are discussed, concentrating on pulse amplification. Early experimental work, as well as the latest results, is presented, and improvements in the SOA design allowing the generation of higher optical pulse energy are discussed.

Keywords: Gallium nitride, GaN, Semiconductor optical amplifier, SOA, Optical pulse generation

1. Introduction

Gallium nitride (GaN)-based optoelectronic devices have attracted significant research interest over the last two decades. Some of these applications, such as light-emitting diodes (LEDs) and ultraviolet (UV),[1] blue-violet, blue, and green laser diodes (LDs), have already been commercialized and have had an impact on everyday life as solid-state lighting, high-capacity optical storage (such as Blu-ray discs), and display units. The GaN-based material AlGaInN has the potential to cover a particularly wide spectral range, from the deep UV to the infrared (IR). LED emissions at wavelengths as short as 210 nm have already been reported [1]. In the

1 375 nm.

case of LDs, lasing actions over the range of 330–350 nm have been obtained with electrical pumping using GaN or AlGaN quantum wells [2, 3]. In addition, Frost et al. reported lasing at longer wavelengths in the red region of the spectrum (at 630 nm) from a InGaN/GaN quantum dot laser [4]. The fact that many researchers have focused on this topic indicates the significant potential of GaN-based optoelectronic devices. However, one important device is missing: the semiconductor optical amplifier (SOA).

An SOA is an important component of optical communication systems, and numerous reports regarding this type of device have been published since its invention in the 1960s. One of the main advantages of the SOA is its ability to be monolithically integrated with other devices. An SOA can be used as a pre-amplifier or a booster amplifier as well as in other functional devices, such as a wavelength converter or optical switch that utilizes its nonlinear nature [5, 6]. An SOA can also be applied as a gain medium to produce short optical pulses in conjunction with a saturable absorber [7]. In high peak power applications, such as two photon bioimaging, an SOA can be used to boost the short optical pulses generated by a mode-locked laser diode (MLLD) [8, 9].

High peak power and ultrashort optical pulses have a number of unique applications, many of which utilize the multiphoton processes that are discussed in detail in Section 4. The majority of pulse sources, however, consist of large, bulky solid-state lasers such as a mode-locked titanium sapphire (Ti:Sap) laser. Moreover, to generate optical pulses at near-UV wavelengths, most of the available pulse sources require wavelength conversion, such that a second- or third-order harmonic of an IR pulse is required. This means that more sophisticated laser systems are necessary to obtain UV pulses. Fiber lasers are an alternative to solid-state lasers and have the advantage of a smaller footprint. However, the requirements for wavelength conversion are the same since these devices can only generate photons in the IR wavelength. Such wavelength conversion systems have a number of disadvantages: a larger footprint, the need for precise alignment, less wall-plug efficiency, and increased complexity of the overall system, usually leading to higher costs and longer stabilizing times. For all these reasons, the direct generation of UV pulses is highly desirable, and thus, a GaN-based SOA could be an important device with regard to obtaining short wavelength optical pulses.

As noted, GaN-based devices potentially can generate a very wide range of photons, from the deep UV to the red wavelength of the spectrum. Optical pulse generation in this type of device was first demonstrated in 1997 by Professor Nakamura, the 2014 Noble laureate, using a self-pulsating LD (SPLD) [10]. Since then, many groups have explored GaN-based lasers with the aim of producing optical pulses. Earlier studies concentrated on self-pulsation for applications in optical storage systems since this approach can reduce the optical feedback noise [1–-14]. Several pulse generation techniques exist, including gain-switching [1–17], self-pulsating [18-20], mode-locking [7, 17, 21], and superradiance [22]. Kono et al. demonstrated the first gain-switching (GS) operation of a GaN-based LD, producing a peak power of 12 W and 10 W with a pulse duration of 10 ps at 405 nm [15, 17]. Kuramoto et al. later improved the peak power to 55 W by optimizing the electron blocking layer in the LD [16]. SPLDs were also explored for applications in high peak power optical sources [18, 20, 23], and results included a peak power of 2.4 W with a bisectional LD [18], 10 W and 0.6 W with a triple section straight

http://dx.doi.org/10.5772/61664

waveguide LD [19, 20], and 20 W and 10 W with a triple section bow tie structure [23, 24]. Mode locking is another means of generating optical pulses and was first demonstrated by Gee and Bowers using a GaN-based SOA as the gain medium [7]. Saito also demonstrated an external cavity passive mode-locked laser diode (MLLD), incorporating a bisectional waveguide structure with a 3-ps pulse duration and a 0.2-W peak power [25]. Oki et al. improved the peak power to 3 W in the optimized active region [26] and later to 20 W by employing a flared waveguide structure [21]. The reduction of the pulse duration is important for high peak power generation, and Kono et al. have demonstrated 200 fs pulse generation using a dispersion compensated external cavity and spectral filtering [27]. To further improve the peak power and pulse energy, the use of an SOA is essential. The SOA can be used to boost the output power generated by an LD in a master oscillator power amplifier (MOPA) configuration. Our group has previously developed GaN-based SOAs meant to improve the pulse energy as well as the peak power. In 2010, a peak power over 100 W with a corresponding pulse energy of approximately 330 pJ was demonstrated, employing an MLLD in conjunction with an SOA [28], and these values were later improved to approximately 300 W and 590 pJ [29]. Recently, an SOA incorporating a widely flared waveguide structure was developed, and the peak power and the pulse energy were further improved to 2.2 nJ and 630 W [30]. The pulse characteristics of published GaN-based devices are summarized in Figure 1 and Table 1 (note that earlier studies of SPLDs were excluded from these summaries since pulse durations were not available). It can be clearly seen that the use of an SOA significantly improves the peak power as well as the pulse energy.

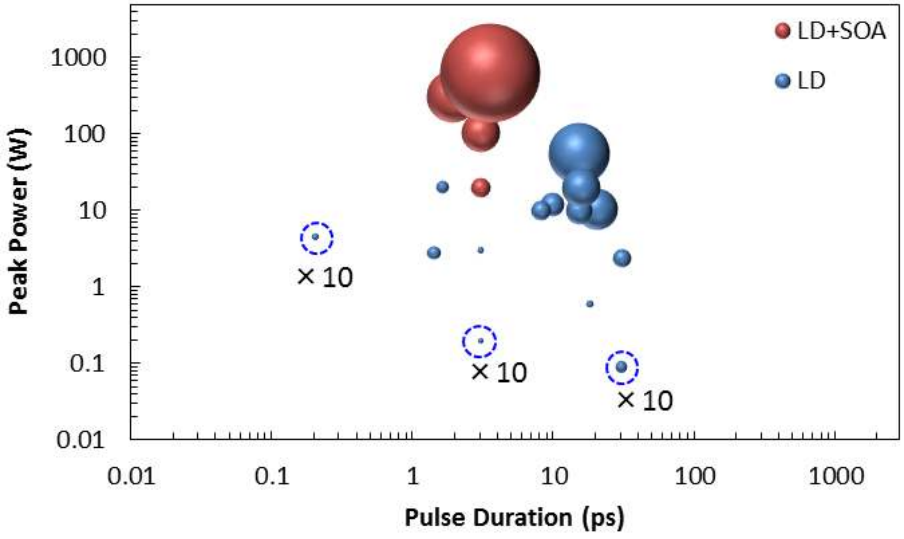

Figure 1. Peak power vs. pulse duration for GaN-based devices. The size of each circle indicates the optical pulse energy. The use of an SOA effectively increases both the peak power and pulse energy. Note that in the case of those data points indicated by dashed circles, the pulse energies are multiplied by 10 for illustrative purposes.

Device type	Pulse Energy (pJ)	Peak Power (W)	Average power (mW)	Pulse Repetition (GHz)	Pulse Duration (ps)	Wavelength (nm)	Reference
Gain-switching LD	116	12	0.01	0.0001	9.7	405	[15]
	820	55	.82	.001	15	401	[16]
Self-pulsating LD	72	2.4	65	0.9	30	407	[18]
	11[1]	0.6	-	4.5	18	414	[19]
	150	10	150	1	15	402	[20]
	80[2]	10	80[1]	1.7	8	-	[24]
	310	20	260	0.84	15.5	406	[23]
Mode-locked LD	2.8	0.09	2	0.72	30	408.5	[7]
	0.6	0.2	0.6	1	3	404.5	[25]
	8.9	3	8.9	3	1	404	[26]
	32	20	32	1	1.6	403.5	[21]
	0.9	4.5	0.9	1	0.2	401	[27]
Mode-locked LD + SOA	78	20	78	1	3	404	[31]
	329	103	329	1	3	404.3	[28]
	586	308	586	1	1.9	405.4	[29]
	2200	630	710	0.812	3.5	405.2	[30]

[1]: Estimated using the peak power, pulse repetition and pulse duration values provided in the paper.

[2]: Estimated by using values provided in the paper

Table 1. Summary of the GaN-based optical pulse sources developed by various research groups.

2. Characterization of continuous wave light amplification

In this section, the basic characteristics of GaN-based SOAs are reviewed.

2.1. Basic structures

In general, there are two types of SOA: the Fabry–Perot type and the travelling-wave type. A Fabry–Perot SOA has nonzero facet reflectivity so that signal light is amplified as the result of many passes through the amplifier. In contrast, a travelling-wave SOA has negligible facet reflectivity such that the signal passes through only once (single-pass). A travelling-wave SOA is simpler to use, and so these devices are discussed exclusively in the present chapter. GaN-based SOAs that we would discuss throughout this chapter consist of a double quantum well structure with $Ga_{0.92}In_{0.08}N$ quantum wells and $Ga_{0.98}In_{0.02}N$ barriers grown on an n-GaN

http://dx.doi.org/10.5772/61664

substrate by metal organic chemical vapor deposition (MOCVD). The layer structure is shown in Figure 2. In a travelling-wave SOA, it is important to minimize facet reflectivity, and this is illustrated in Figure 3. Both devices shown in this figure are ridge waveguide structures with a length of 1 mm and both incorporate facets with anti-reflection (AR) coatings. Waveguides are straight (Figure 3(a)) and angled by 5° (Figure 3(b)). As the result of nonzero reflectivity, the straight waveguide exhibits significant resonance and a multilongitudinal mode, both of which are undesirable with regard to SOA operation. The incorporation of the angled waveguide effectively reduces back reflection from the facets and thus suppresses the resonance effect.

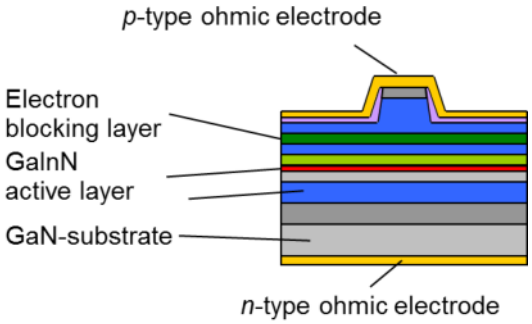

Figure 2. Schematics of the layer structure of the SOAs discussed in the present chapter.

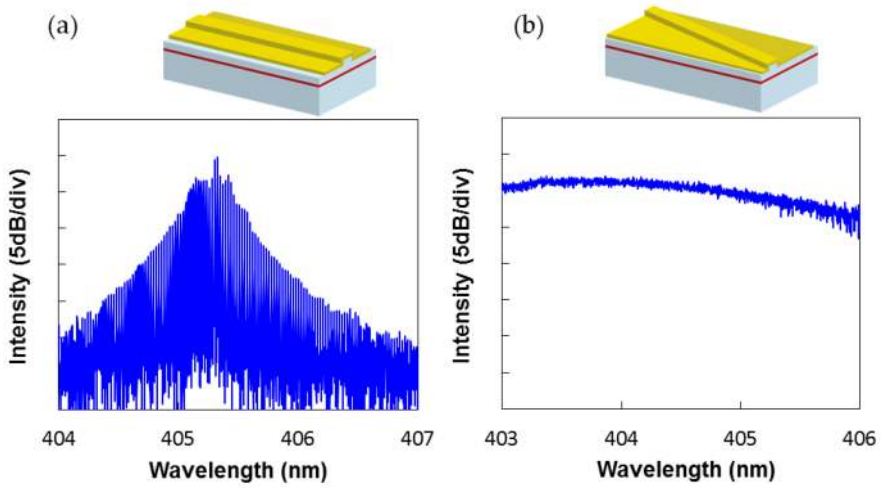

Figure 3. Optical spectra obtained from 1 mm long SOAs with either (a) straight or (b) angled waveguides. Although both structures had AR-coated faces, the straight waveguide exhibits strong resonance due to residual reflections from an imperfect AR coating.

The output power of an SOA is limited by its saturation power, P_{sat}, which is given by

$$P_{\text{sat}} = \frac{h\nu dw}{\Gamma a \tau} \tag{1}$$

where h is the Plank constant, ν is the signal optical frequency, d and w are the active region thickness and width, respectively, Γ is the confinement factor, a is the differential gain, and τ is the carrier lifetime. Equation (1) indicates that a larger active region cross section, a lower confinement factor, a lower differential gain, and a reduced carrier lifetime are desirable for high power applications. However, the output power is independent of device length. Equation (1) can be interpreted qualitatively, that is, the amount of energy that can be stored in the device is important for higher output from the SOA.

The basic amplification characteristics of an SOA were assessed using device A shown in Figure 4, incorporating a flared waveguide. The input and the output waveguide widths were 1.4 and 5 μm, respectively, and both facets were AR coated. As noted earlier, the waveguide was angled at 5° to suppress the resonance effect.

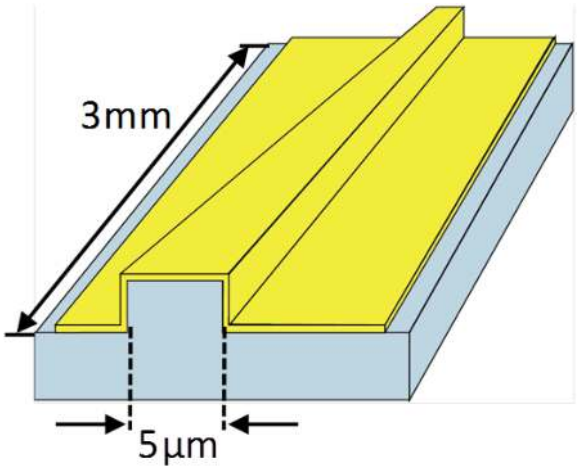

Figure 4. Schematics of device A.

2.2. Continuous wave amplification characteristics

In the amplification of continuous-wave (CW) light by the SOA, device A was assessed using the experimental setup shown in Figure 5. The resulting net gain (sometimes also known as the fiber-to-fiber gain) and output power at an input wavelength of 404 nm are presented as functions of input power at operating currents of 3, 4, and 5 kA/cm^2 in Figure 6. The net gain values were estimated using an optical band-pass filter (BPF) to reject the out-of-band

http://dx.doi.org/10.5772/61664

components of the amplified spontaneous emission (ASE). It should be noted that the net gain values in this figure include the input and output coupling losses. It is evident that a gain of over 20 dB was obtained from a small signal input of less than 1 mW, a result that is comparable to the performance of SOAs fabricated with other materials [5, 6].

Wavelength dependencies were characterized by tuning the input wavelength to 403, 405, or 407 nm, and the corresponding spectra are presented in Figure 7, in which very different spectra are observed at different input wavelengths. At the shorter wavelength, the amplified spectrum shows that ASE is present, whereas less ASE is observed from amplification at longer wavelengths of 405 and 407 nm. Figure 8(a) plots the output power and ASE spectra, while Figure 8(b) presents the net gain spectra obtained at different input powers. It is interesting to note that the gain peak shifts to longer wavelength as the input power is increased. At lower input power, the wavelength of the gain peak and the maximum output power are nearly equal to the ASE peak, while higher input power results in a red shift of these values. This phenomenon can possibly be explained by considering that gain saturation due to carrier depletion leads to intra-band relaxation of the carriers. This results in more carriers available for longer wavelength amplification. In addition, GaN-based systems are known to have higher effective masses of electrons and holes [32, 33], and this may also play a role in this mechanism.

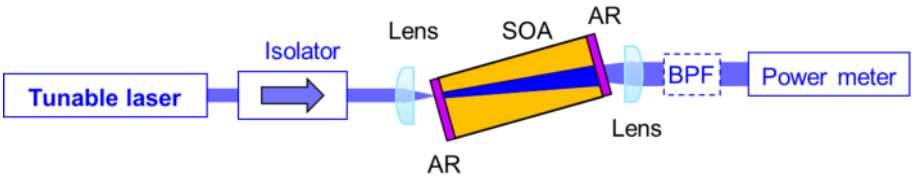

Figure 5. Experimental setup for CW amplification.

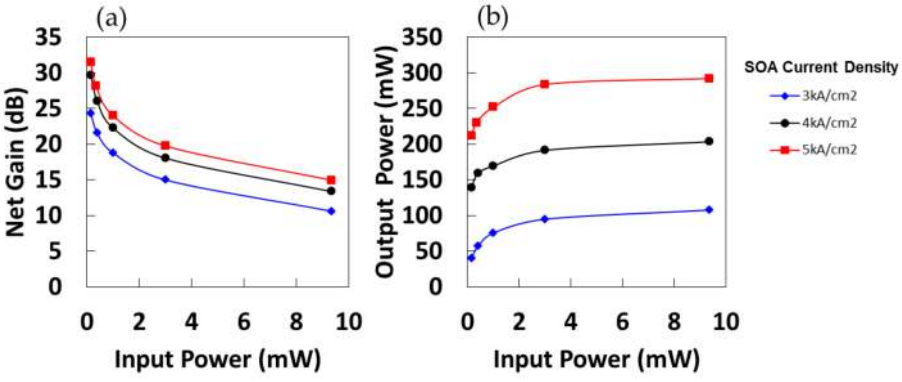

Figure 6. Net gain (left) and output power (right) obtained from the SOA (device A) as functions of CW input power for current densities of 3, 4, and 5 kA/cm^2 at an input wavelength of 404 nm.

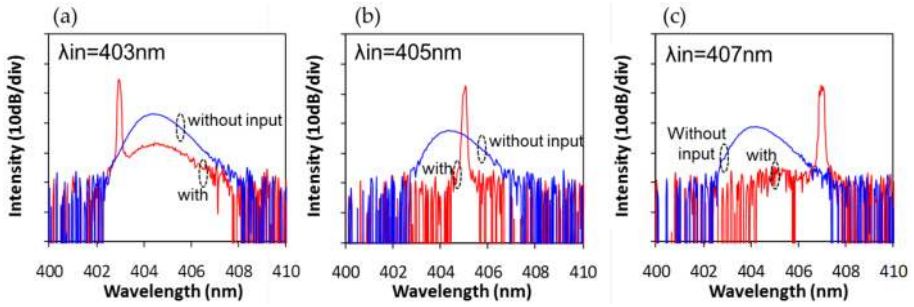

Figure 7. Optical spectra of the output of an angled SOA obtained with input wavelengths of (a) 403, (b) 405, and (c) 407 nm. Current density and input power were 4 kA/cm^2 and 11 mW, respectively. Spectra with (red) and without (blue) input are shown for each wavelength.

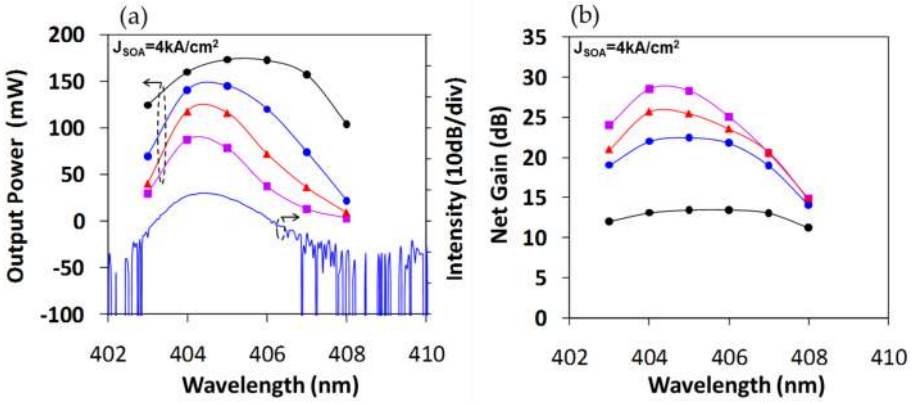

Figure 8. (a) Output power and ASE spectra and (b) net gain spectra obtained from device A at input powers of 11 mW (black), 1.2 mW (blue), 0.4 mW (red), and 0.2 mW (violet).

3. Pulse amplification

3.1. Limiting factor

Pulse amplification was initially studied using device A [31], employing a GaN-based external cavity MLLD developed by our group [26]. In this work, a GaN-based LD having the same GaInN active region as the SOA was grown by MOCVD. The resulting LD chip was composed of a forward bias gain section and a reverse bias saturable absorption (SA) section. The facets had a high reflection coating on the SA side and an AR coating on the other side. More details regarding this MLLD are available in the literature [26]. Figure 9 shows the output power of the device as a function of the average input power for both CW and pulse inputs at a 3-

kA/cm^2 SOA bias current density. From this figure, it is evident that significantly lower average power was obtained when applying pulse amplification. To investigate the limiting factors for pulse amplification, we acquired optical spectra as well as temporal characteristics using an optical spectrum analyzer (OSA) and a streak camera. Figure 10(a) presents the optical spectra and Figure 10(b) shows streak camera images obtained from amplified pulses at 2 and 4 kA/cm^2 SOA bias current densities. The optical spectra of the amplified pulses exhibit a peak wavelength shift toward longer wavelengths as well as an oscillatory structure, representing self-phase modulation (SPM) [34]. High peak power optical pulses induce carrier depletion, which in turn varies the refractive index. At the lower current density of 2 kA/cm^2, the streak camera image shows clean optical pulses at a repeat rate of 1 GHz. In contrast, at the higher current density (4 kA/cm^2), ASE appears between pulses. The optical spectra also changes at the higher current density, such that a broad fifth peak appears near 403 nm. Careful examination of this short wavelength peak using the streak camera indicated that it is a combination of ASE and pulse elements. The carrier recovery time was determined to be less than 300 ps, and thus significantly faster than the pulse repetition of 1 ns. The duration of the amplified pulse was 3 ps and the peak power was estimated to be only 20 W.

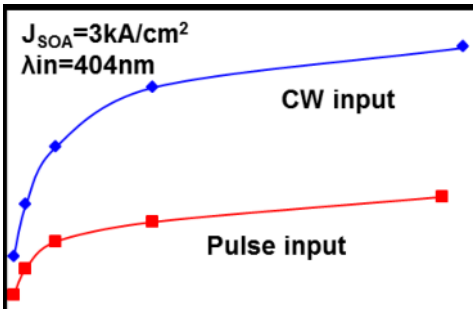

Figure 9. Average output power of the SOA (device A) as a function of input power for CW (diamonds) and pulse (squares) inputs at an SOA current density of 3 kA/cm^2 and an input wavelength of 404 nm. Significant reduction of gain is observed for pulse amplification.

3.2. Improving peak power

Investigation of device A indicated that intense ASE appeared as the operating current density was increased. Intense ASE leads to gain depletion, preventing efficient amplification of optical pulses. In this process, carrier depletion occurring via a stimulated emission process is induced by the intense ASE, which in turn results in fewer carriers available for pulse amplification. This generates the limited peak power of only 20 W. The fact that intense ASE is a limiting factor for an SOA has also been noted in previous studies of other systems, both theoretically and experimentally [35-37]. To overcome this limitation, intense ASE has to be reduced. However, a trade-off exists since ASE is also needed for optical gain. We have thus pursued the development of SOAs by optimizing device structures so as to obtain low ASE while maintaining sufficient gain. Peak powers were improved to approximately 100 W and later to

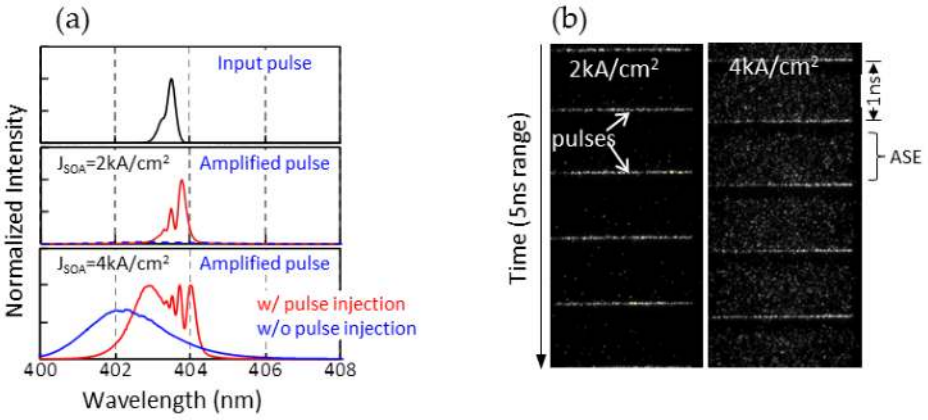

Figure 10. (a) Optical spectra obtained with input and amplified output and (b) streak camera images at SOA current densities of 2 and 4 kA/cm^2. At the higher current density, intense ASE is observed between pulses.

300 W by optimizing device structure such as the length and optical confinement factors [28, 29]. The corresponding optical pulse energies were approximately 330 and 590 pJ. Recently, further improvements gave a pulse energy of 2200 pJ (corresponding to a peak power of 630 W) [30]. This is the highest ever pulse energy reported for a GaN-based all-semiconductor pulse source. Details of this latest device are presented in the following sections. The SOAs described above are illustrated in Figure 11 as devices B, C, and D. It is known that optical pulse amplification is governed by the saturation energy, E_{sat}, of the SOA [34], and that it can be expressed as follows.

$$E_{sat} = \frac{h\nu dw}{\Gamma a} \tag{2}$$

The parameters d, w, and Γ can be readily tuned by adjusting the epitaxial layer structure and waveguide design. In the case of devices B, C, and D, the values of dw/Γ are 8×10^3, 9×10^3, and 6×10^4 μm^2, respectively. Each of these devices was grown by MOCVD, and all have a ridge waveguide structure. Both B and C employ waveguides that are linearly tapered from 1.4 μm at the input facet to 15 μm at the output facet. In the case of D, the waveguide consists of two sections: the straight preamplifier and the flared main amplifier sections. The lengths are 2, 2.5, and 3 mm for B, C, and D, respectively, and more detailed descriptions have been previously published [2-–30]. Figure 12 summarizes the net gain and ASE power values as functions of the SOA current density. For each sample, the net gain is seen to increase with current density but to saturate as the ASE becomes too high. It should be noted that this discussion is not intended to offer a detailed comparison between the devices since the operating conditions under which these data were collected, such as temperature, input pulse width, and power, were not all the same. Rather, the intention is to show the effectiveness of

http://dx.doi.org/10.5772/61664

varying the parameter dw/Γ, which governs the optical pulse energy. Figure 13 plots the optical pulse energy as a function of this term.

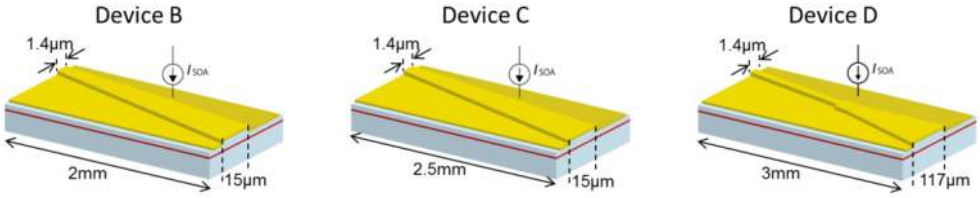

Figure 11. Schematics of three additional SOA designs. The peak power and pulse energy values were approximately 100, 300, and 630 W and 330, 590, and 2200 pJ for devices B, C, and D, respectively.

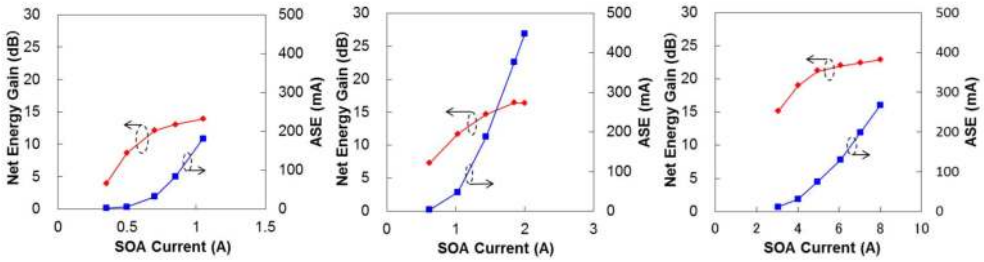

Figure 12. Net gain and ASE power values as functions of SOA current for devices B, C, and D.

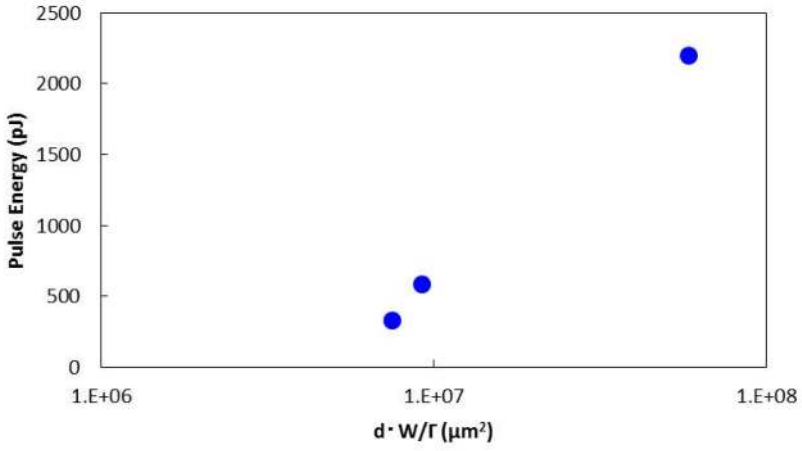

Figure 13. Pulse energy as a function of dw/Γ.

It is helpful to discuss in detail the result obtained with device D. This device employed a passively mode-locked GaN laser as the master oscillator, in the commonly used Littrow configuration. The gain section of the LD was forward biased by 90 mA, and the SA section was reverse biased at –9 V. The pulse repetition rate was 812 MHz, and the input power was 7.2 mW. The wavelength was tuned to 405 nm. Temporal characterization of the input pulse was performed using an in-house intensity autocorrelation measurement apparatus that utilizes the surface second harmonics of a β-BaB_2O_4 (BBO) crystal [38]. Autocorrelation measurements indicated an FWHM value of 4.2 ps, corresponding to a 3.0-ps pulse duration assuming a Gaussian waveform. The peak power was estimated to be 3 W.

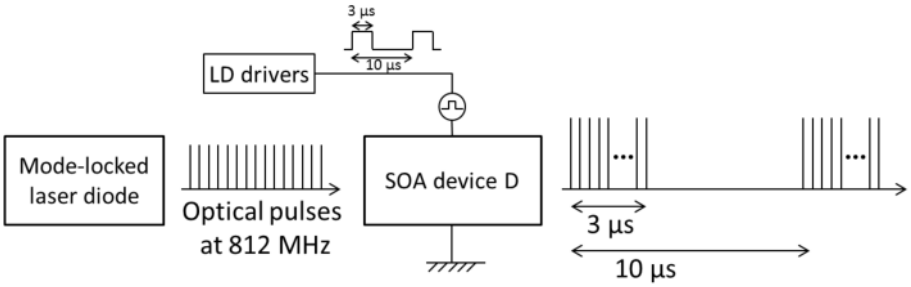

Figure 14. Schematics of the master oscillator power amplifier using SOA device D.

SOA D was driven by LD drivers at a 100-kHz repetition rate with 3 μs width rectangular current pulse, as illustrated in Figure 14, which presents the autocorrelation trace and optical spectrum acquired at a 8-kA/cm^2 bias current density. Here, the FWHM was 5.0 ps, and the pulse duration was estimated to be 3.5 ps, assuming a Gaussian waveform. Even though a high net gain of greater than 20 dB was obtained, the pulse duration was not significantly broadened. The peak wavelength of the amplified pulse was 405.2 nm, indicating a 0.2-nm red shift, as shown in Figure 15(b). The spectral bandwidth also increased from 0.08 to 0.26 nm after amplification. These spectral changes were due to SPM. It is important to point out that the amount of red shift exhibited in this case was less than that observed in previous trials; as an example, a shift of 0.4 nm was obtained with device C [29]. Figure 16 shows the average output power and estimated pulse energy values as functions of the SOA bias current density. The average output power values were 0.71 and 0.27 W with and without pulse injection. At 8 kA/cm^2, the pulse energy was estimated to be 2.2 nJ, and the corresponding peak power was estimated to be 630 W. These are the highest pulse energy and peak power ever generated by GaN-based MOPA.

4. Potential applications

There are many potential applications for GaN-based SOAs, among which those utilizing optical pulses are the most prominent. In this section, these applications are discussed.

http://dx.doi.org/10.5772/61664

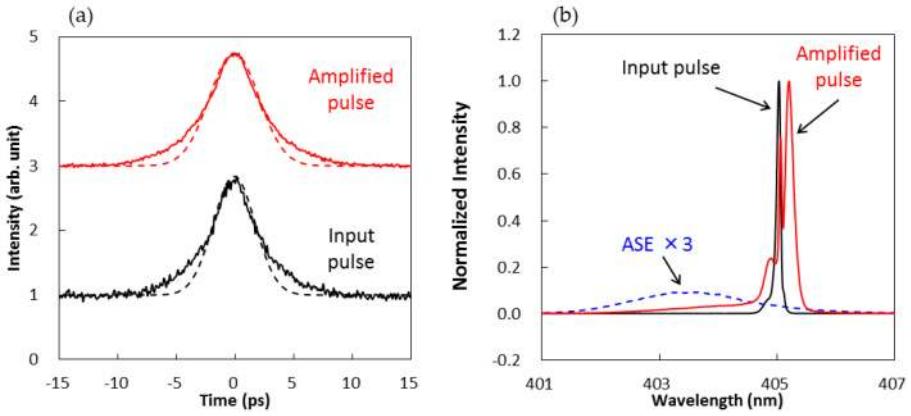

Figure 15. (a) Autocorrelation traces and (b) optical spectra of input and amplified pulses. The dashed lines show Gaussian function fitted to the autocorrelation traces in panel a. The ASE spectrum (with its intensity multiplied by three for illustrative purposes) is also shown in panel b as a dashed line.

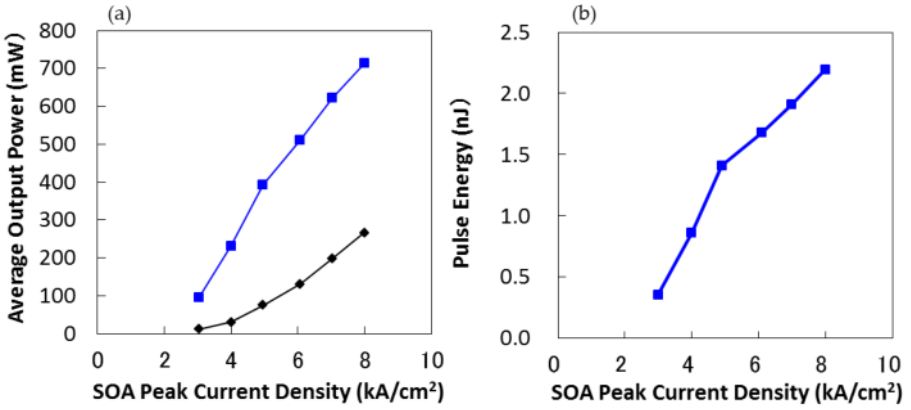

Figure 16. (a) Average output and (b) pulse energy values as functions of the SOA bias current density.

4.1. Micromachining applications

Recently, there has been a rapid growth in laser material processing, as the cost of lasers has decreased and fiber laser technology has advanced. In microscale machining, short optical pulses are desirable since picosecond/femtosecond pulses can effectively reduce the heat damage resulting from the laser light. In fact, it has been demonstrated that nanosecond pulses produce dull edges [39], as shown by Chichkov et al., who demonstrated this by comparing the pulse width dependence of laser ablation of steel.

Short wavelength optical pulses can also be beneficial with regard to precise processing since the spot size of the focused beam is proportional to NA/λ, where NA is the numerical aperture

of the lens and λ is the wavelength of the laser. Kauf et al. published a systematic study of microprocessing using mode-locked picosecond and q-switched nanosecond UV lasers having the same average and peak power values, although with differing pulse energies [40]. These trials demonstrated that picosecond UV pulses offer an advantage compared to nanosecond pulses since they allow higher cutting speeds when working with dielectric materials such as polyimides. The significantly higher pulse repetition of the mode-locked laser operating at 80 MHz resulted in a higher cutting speed compared to that obtained from the q-switched laser working at 80 Hz.

4.2. Orthoptics

Laser refractive surgery, such as laser in situ keratomileusis (LASIK), corrects the refractive properties of the cornea. Two different types of pulse lasers are typically used in LASIK: an IR femtosecond laser for cutting corneal flaps and a UV nanosecond excimer laser for ablating corneal tissue. Ablation of the corneal tissue with UV pulses (typically at 193 nm) is able to change the shape of the cornea's surface to allow for vision correction. Recently, an alternative method for vision correction was demonstrated by Xu and Knox et al. Instead of physically removing a part of cornea, this new noninvasive technique modifies the refractive index of the cornea using femtosecond pulses at 400 nm, which is the most effective wavelength. The 400-nm pulses are provided by the second-order harmonics of a mode-locked Ti:Sap laser with an average power of 60 ± 1 mW and corresponding pulse energies of approximately 0.8 nJ at the cornea. A GaN-based SOA employing MLLD would seem to be a promising candidate for this application since the required average power and pulse energies can easily be generated by the type of SOA discussed in the present chapter and the associated semiconductor-based system offers energy efficiency and compactness.

4.3. Optical storage

The storage capacities of optical disks have improved from 0.7 gigabytes (GB) in the case of compact discs (CDs) to 4.7 GB for digital versatile discs (DVDs) and, more recently, to 25 GB with Blu-ray discs. These improvements were realized in conjunction with advances in laser diode technologies in terms of achieving shorter lasing wavelengths since the spot size of the laser beam is proportional to λ/NA. For next-generation optical data storage, three-dimensional (3D) optical data storage might be the best candidate since, as the name implies, this technique allows information to be stored three dimensionally, generating a significant increase in storage capacity [41]. Several groups have demonstrated such systems [42, 43], and 1 terabyte data storage has been demonstrated [44]. To store data three dimensionally, multiphoton processes, such as two photon absorption, must be induced using high peak power optical pulses. A GaN-based SOA incorporating MLLD would be highly suitable as a practical pulse source, and in fact, such applications have already been demonstrated [45, 46].

http://dx.doi.org/10.5772/61664

5. Conclusion

GaN-based optoelectronic devices are already widely used as optical storage lasers and solid-state lighting, and because of their ability to potentially cover a wide spectral range from the deep UV to the IR regions, many research studies concerning these devices are ongoing. However, very few reports on GaN-based SOAs exist. In this chapter, the basic characteristics of GaN-based SOAs were reviewed, focusing on pulse amplification. The particular SOA devices described herein generate a pulse energy greater than 2 nJ, a value that is comparable to the values obtained from widely used pulse sources based on solid-state lasers. There are many potential applications for these devices, such as microprocessing, orthoptics, and high-density optical storage, using UV picosecond and femtosecond pulses. These applications would all benefit from employing GaN-based SOAs.

Acknowledgements

The authors wish to gratefully acknowledge Professor Yokoyama of Tohoku University for helpful discussions and to note that earlier studies of the GaN-SOAs (devices A, B, and C) were performed in collaboration with Professor Yokoyama's research group. Thanks are also due to the author's research colleagues: T. Oki, Y. Takiguchi, M. Kuramoto, T. Miyajima, H. Nakajima, M. Shiozaki, Y. Hanzawa, N. Sugawara, and M. Ikeda. Finally, the assistance of Sony Semiconductor in fabricating the experimental devices is gratefully acknowledged.

Author details

Rintaro Koda*, Hideki Watanabe and Shunsuke Kono

*Address all correspondence to: Rintaro.Koda@jp.sony.com

Semiconductor Device Development Division, Sony Corporation, Japan

References

[1] Taniyasu Y, Kasu M, Makimoto T: An aluminium nitride light-emitting diode with a wavelength of 210 nanometres. Nature. 2006;441(7091):32-–8.

[2] Yamashita Y, Kuwabara M, Torii K, Yoshida H: A 340-nm-band ultraviolet laser diode composed of GaN well layers. Optics Express. 2013;21:3133.

[3] Yoshida H, Yamashita Y, Kuwabara M, Kan H: Demonstration of an ultraviolet 336 nm AlGaN multiple-quantum-well laser diode. Applied Physics Letters. 2008;93(24): 241106.

[4] Frost T, Banerjee A, Sun K, Chuang SL, Bhattacharya P: InGaN/GaN quantum dot red (λ = 630 nm) laser. IEEE Journal of Quantum Electronics. 2013;49:923.

[5] Connelly MJ. Semiconductor Optical Amplifiers: Springer US; 2007.

[6] Dutta NK, Wang Q. Semiconductor Optical Amplifiers: World Scientific Pub.; 2006.

[7] Gee S, Bowers JE: Ultraviolet picosecond optical pulse generation from a mode-locked InGaN laser diode. Applied Physics Letters. 2001;79:1951.

[8] Ding Y, Aviles-Espinosa R, Cataluna MA, Nikitichev D, Ruiz M, Tran M, et al.: High peak-power picosecond pulse generation at 1.26 μm using a quantum-dot-based external-cavity mode-locked laser and tapered optical amplifier. Optics Express. 2012;20(13):14308–20.

[9] Kuramoto M, Kitajima N, Guo H, Furushima Y, Ikeda M, Yokoyama H: Two-photon fluorescence bioimaging with an all-semiconductor laser picosecond pulse source. Optics Letters. 2007;32(18):2726–8.

[10] Nakamura S, Masayuki Senoh, Nagahama S-i, Iwasa N, Yamada T, Matsushita T, et al.: InGaN/GaN/AlGaN-based laser diodes with modulation-doped strained-layer superlattices. Japanese Journal of Applied Physics. 1997;36:L1568.

[11] Obata T, Kitajima N, Ohta M, Ichinokura H, Masaru K: Low noise characteristics of AlGaInN-based self-pulsating laser diodes. Physica Status Solidi (A). 2008;205:1096.

[12] Ohno T, Ito S, Kawakami T, Taneya M: Self-pulsation in InGaN laser diodes with saturable absorber layers. Applied Physics Letters. 2003;83:1098.

[13] Tronciu VZ, Yamada M, Abram RA: Analysis of the dynamics of a blue-violet inxGa1-xN laser with a saturable absorber. American Physical Society. 2004;70(22): 026604-1-6.

[14] Tronciu VZ, Yamada M, Ohno T, Ito S, Kawakami T, Taneya M: Self-pulsation in an InGaN laser-theory and experiment. IEEE Journal of Quantum Electronics. 2003;39(12):1509–14.

[15] Kono S, Oki T, Miyajima T, Ikeda M, Yokoyama H: 12W peak-power 10ps duration optical pulse generation by gain switching of a single-transverse-mode GaInN blue laser diode. Applied Physics Letters. 2008;93(13):131113.

[16] Kuramoto M, Oki T, Sugahara T, Kono S, Ikeda M, Yokoyama H: Enormously high-peak-power optical pulse generation from a single-transverse-mode GaInN blue-violet laser diode. Applied Physics Letters. 2010;96(5):051102.

[17] Oki T, Kono S, Kuramoto M, Ikeda M, Yokoyama H: Generation of over 10-W peak-power picosecond pulses by a gain-switched AlGaInN-based self-pulsating laser diode. Applied Physics Express. 2009;2:032101.

[18] Miyajima T, Watanabe H, Ikeda M, Yokoyama H: Picosecond optical pulse generation from self-pulsating bisectional GaN-based blue-violet laser diodes. Applied Physics Letters. 2009;94(16):161103.

[19] Scheibenzuber WG, Hornuss C, Schwarz UT, Sulmoni L, Dorsaz J, Carlin J-F, et al.: Self-pulsation at zero absorber bias in GaN-based multisection laser diodes. Applied Physics Express. 2011;4(6):062702.

[20] Watanabe H, Miyajima T, Kuramoto M, Ikeda M, Yokoyama H: 10-W peak-power picosecond optical pulse generation from a triple section blue-violet self-pulsating laser diode. Applied Physics Express. 2010;3(5):052701.

[21] Oki T, Koda R, Kono S, Miyajima T, Watanabe H, Kuramoto M, et al.: Direct generation of 20 W peak power picosecond optical pulses from an external-cavity mode-locked GaInN laser diode incorporating a flared waveguide. Applied Physics Letters. 2011;99(11):111105.

[22] Olle VF, Vasil'ev PP, Wonfor A, Penty RV, White IH: Ultrashort superradiant pulse generation from a GaN/InGaN heterostructure. Opt Express. 2012;20(7):7035–9.

[23] Watanabe H, Kuramoto M, Kono S, Ikeda M, Yokoyama H: Blue-violet bow-tie self-pulsating laser diode with a peak power of 20 W and a pulse energy of 310 pJ. Applied Physics Express. 2010;3(12):122103.

[24] Holc K, Weig T, Köhler K, Wagner J, Schwarz UT: Impact of band structure and absorber dynamics on self-Q-switching in GaN-based multisection laser diodes at high reverse bias. Applied Physics Express. 2013;6(8):084101.

[25] Saito K, Watanabe H, Miyajima T, Ikeda M, Yokoyama H: Mode locking of an external-cavity bisection GaInN blue-violet laser diode producing 3 ps duration optical pulses. Applied Physics Letters. 2010;96(3):031112.

[26] Oki T, Saito K, Watanabe H, Miyajima T, Kuramoto M, Ikeda M, et al.: Passive and hybrid mode-locking of an external-cavity GaInN laser diode incorporating a strong saturable absorber. Applied Physics Express. 2010;3(3):032104.

[27] Kono S, Watanabe H, Koda R, Miyajima T, Kuramoto M: 200-fs pulse generation from a GaInN semiconductor laser diode passively mode-locked in a dispersion-compensated external cavity. Applied Physics Letters. 2012;101(8):081121.

[28] Koda R, Oki T, Miyajima T, Watanabe H, Kuramoto M, Ikeda M, et al.: 100 W peak-power 1 GHz repetition picoseconds optical pulse generation using blue-violet GaInN diode laser mode-locked oscillator and optical amplifier. Applied Physics Letters. 2010;97(2):021101.

[29] Koda R, Oki T, Kono S, Miyajima T, Watanabe H, Kuramoto M, et al.: 300 W peak power picosecond optical pulse generation by blue-violet GaInN mode-locked laser diode and semiconductor optical amplifier. Applied Physics Express. 2012;5(2): 022702.

[30] Koda R, Takiguchi Y, Kono S, Watanabe H, Hanzawa Y, Nakajima H, et al.: Generation of a 2.2 nJ picosecond optical pulse with blue-violet wavelength using a GaInN master oscillator power amplifier. Submitted to Applied Physics Letters. 2015.

[31] Koda R, Oki T, Miyajima T, Watanabe H, Kuramoto M, Ikeda M, et al., editors. Generation and amplification of 400 nm band picosecond optical pulses by GaInN laser diodes. International Conference on Ultrafast Phenomena; 2010 2010/07/18; Snowmass Village, Colorado: Optical Society of America.

[32] Coldren LA, Corzine SW. Diode Lasers and Photonic Integrated Circuits. Wiley; 1995.

[33] Piprek J. Nitride Semiconductor Devices: Principles and Simulation: Wiley; 2007.

[34] Agrawal GP, Olsson NA: Self-phase modulation and spectral broadening of optical pulses in semiconductor laser amplifiers. IEEE Journal of Quantum Electronics. 1989;25(11):2297–306.

[35] Baveja PP, Maywar DN, Kaplan AM, Agrawal GP: Self-phase modulation in semiconductor optical amplifiers: impact of amplified spontaneous emission. IEEE Journal of Quantum Electronics. 2010;46(9):1396–403.

[36] Brosson P: Analytical model of a semiconductor optical amplifier. Journal of Lightwave Technology. 1994;12(1):49–54.

[37] Lee CH, Delfyett PJ: Limits on amplification of picosecond pulses by using semiconductor laser traveling-wave amplifiers. IEEE Journal of Quantum Electronics. 1991;27(5):1110–4.

[38] Kono S, Oki T, Kuramoto M, Ikeda M, Yokoyama H: Intensity autocorrelation measurement of 400 nm picosecond optical pulses from a GaInN mode-locked semiconductor laser diode using surface second harmonic generation of β-BaB2O4 crystal. Applied Physics Express. 2010;3(12):122701.

[39] Chichkov BN: Femtosecond, picosecond and nanosecond laser ablation of solids. Applied Physics A. 1996;63(2):109–15.

[40] Kauf M, Patel R, Bovatsek J, Gries W: High power UV q-switched and mode-locked laser comparisons for industrial processing applications. Proceedings of SPIE. 2008;6871:687123-10.

[41] Gu M, Li X: The road to multi-dimensional bit-by-bit optical data storage. Optics and Photonics News. 2010;21(7):28–33.

[42] Parthenopoulos DA, Rentzepis PM: Three-dimensional optical storage memory. Science. 1989;245(4920):843–5.

[43] Strickler JH, Webb WW: Three-dimensional optical data storage in refractive media by two-photon point excitation. Optics Letters. 1991;16(22):1780–2.

[44] Walker E, Dvornikov A, Coblentz K, Rentzepis P: Terabyte recorded in two-photon 3D disk. Applied Optics. 2008;47(22):4133–9.

[45] Tashiro S, Takemoto Y, Yamatsu H, Miura T, Fujita G, Iwamura T, et al.: Volumetric optical recording using a 400 nm all-semiconductor picosecond laser. Applied Physics Express. 2010;3(10):102501.

[46] Tashiro S, Yamatsu H, Takemoto Y, Fujita G, Miura T, Iwamura T, et al.: Volumetric optical recording with void marks using an all-semiconductor picosecond laser. Japanese Journal of Applied Physics. 2011;50(9):09MF3.